Examination of XMM-Newton spectra of the SNR 0509-67.5

D. Kosenko
J.Vink
S.Blinnikov
A.Rasmussen

Astronomical Institute Utrecht

X-ray Universe, Granada, May 28, 2008

The benefits

- The SNR extension — 25", which makes it a good target for the XMM grating spectrometer
- Distance to the LMC — 50 kpc $\Rightarrow$ $R_{\rm SNR} = 3.6$ pc
- Interstellar absorption in the direction of the LMC is lower than for the Galactic remnants

The benefits

- The SNR extension — 25", which makes it a good target for the XMM grating spectrometer
- Distance to the LMC — 50 kpc ⇒ $R_{\rm SNR} = 3.6$ pc
- Interstellar absorption in the direction of the LMC is lower than for the Galactic remnants

The benefits

- The SNR extension — 25", which makes it a good target for the XMM grating spectrometer
- Distance to the LMC — 50 kpc $\Rightarrow \quad R_{\mathrm{SNR}} = 3.6$ pc
- Interstellar absorption in the direction of the LMC is lower than for the Galactic remnants

Outline of the data available

Chandra data:

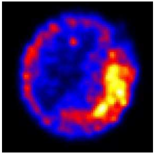

0.45-1.8 keV

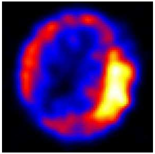

1.8-2.5 keV

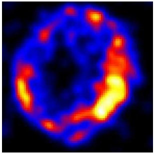

2.5-6.0 keV

Some facts:

- Warren & Hughes (2004);
  $n_{\rm CSM} \simeq 0.05~{\rm cm}^{-3}$,
  metal-rich,
  SNIa explosion - DD
- Badenes et al (2008);
  $n_{\rm CSM} \simeq 0.4~{\rm cm}^{-3}$,
  $t \simeq 400$ years,
  SNIa explosion - DD
  ($M_{\rm Ni} = 0.97\,M_\odot$ $E = 1.4 \times 10^{51}$ ergs)
- Rest et al (2005);
  $t = 400 \pm 120$ years
- Vink 2006; Ghavamian et al 2007; Rest et al 2008; etc...

Outline of the data available

Chandra data:

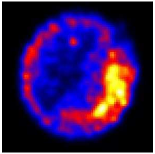

0.45-1.8 keV

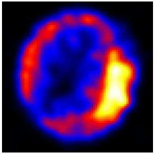

1.8-2.5 keV

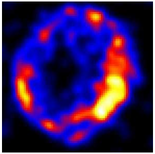

2.5-6.0 keV

Some facts:

- Warren & Hughes (2004);
  $n_{\rm CSM} \simeq 0.05\ {\rm cm}^{-3}$,
  metal-rich,
  SNIa explosion - DD
- Badenes et al (2008);
  $n_{\rm CSM} \simeq 0.4\ {\rm cm}^{-3}$,
  $t \simeq 400$ years,
  SNIa explosion - DD
  ($M_{\rm Ni} = 0.97\, M_{\odot}$ $E = 1.4 \times 10^{51}$ ergs)
- Rest et al (2005);
  $t = 400 \pm 120$ years
- Vink 2006; Ghavamian et al 2007; Rest et al 2008; etc...

Outline of the data available

Chandra data:

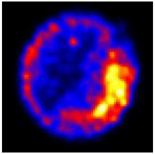

0.45-1.8 keV

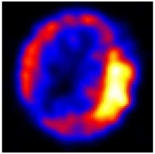

1.8-2.5 keV

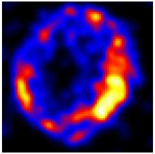

2.5-6.0 keV

Some facts:

- Warren & Hughes (2004);
  $n_{\rm CSM} \simeq 0.05\ {\rm cm}^{-3}$,
  metal-rich,
  SNIa explosion - DD
- Badenes et al (2008);
  $n_{\rm CSM} \simeq 0.4\ {\rm cm}^{-3}$,
  $t \simeq 400$ years,
  SNIa explosion - DD
  ($M_{\rm Ni} = 0.97\, M_\odot$ $E = 1.4 \times 10^{51}$ ergs)
- Rest et al (2005);
  $t = 400 \pm 120$ years
- Vink 2006; Ghavamian et al 2007; Rest et al 2008; etc...

EPIC MOS and RGS spectra of the SNR

First approach:
fitting with SPEX (Kaastra et al, 1996, up-to-date atomic data)

single $n_e t$ NEI fit

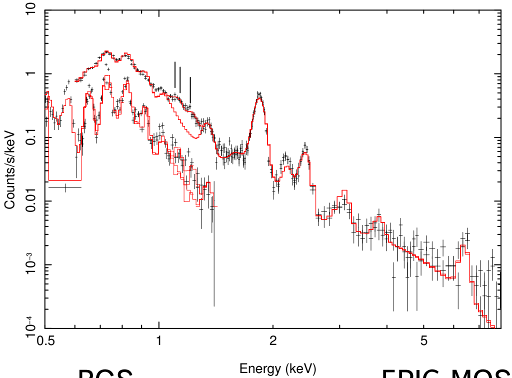

RGS EPIC MOS

The Fe K feature (6.5 keV) — separately: low ionized iron with $n_e t \simeq 10^9$ s/cm^3 $\Rightarrow$ Swept up iron $\sim 0.05\, M_\odot$

EPIC MOS and RGS spectra of the SNR

First approach:
fitting with SPEX (Kaastra et al, 1996, up-to-date atomic data)

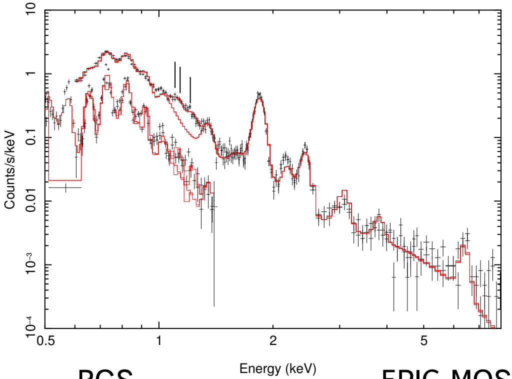

RGS EPIC MOS

single $n_e t$ NEI fit

The Fe K feature (6.5 keV) — separately: low ionized iron with $n_e t \simeq 10^9$ s/cm^3 $\Rightarrow$ Swept up iron $\sim 0.05\,M_\odot$

EPIC MOS and RGS spectra of the SNR

First approach:
fitting with SPEX (Kaastra et al, 1996, up-to-date atomic data)

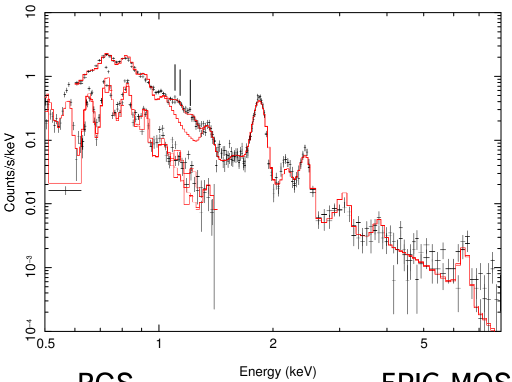

RGS EPIC MOS

single $n_e t$ NEI fit

The Fe K feature (6.5 keV) — separately: low ionized iron with $n_e t \simeq 10^9$ s/cm^3 $\Rightarrow$ Swept up iron $\sim 0.05\,M_\odot$

The SNR parameters from the fitting

Parameter	NEI, MOS+RGS	NEI+pow, MOS+RGS
$n_e n_H V \times 10^{58}$, cm^{-3}	$1.15^{+0.12}_{-0.12}$	$0.55^{+0.15}_{-0.16}$
kT, keV	$4.01^{+0.23}_{-0.18}$	$4.55^{+0.22}_{-0.20}$
$n_e t \times 10^{10}$, $\mathrm{s/cm}^3$	$1.41^{+0.03}_{-0.03}$	$1.63^{+0.04}_{-0.04}$
$\chi^2/d.o.f.$	2.61	2.29

- Power index $\Gamma = 3.5 \pm 0.1$
- $\{EM \quad \text{and} \quad R \simeq 3.6 \text{ pc}\} \Rightarrow n_{\rm CSM} \lesssim 0.6 \text{ cm}^{-3}$

The SNR parameters from the fitting

Parameter	NEI, MOS+RGS	NEI+pow, MOS+RGS
$n_e n_H V \times 10^{58}$, cm^{-3}	$1.15^{+0.12}_{-0.12}$	$0.55^{+0.15}_{-0.16}$
kT, keV	$4.01^{+0.23}_{-0.18}$	$4.55^{+0.22}_{-0.20}$
$n_e t \times 10^{10}$, $\mathrm{s/cm^3}$	$1.41^{+0.03}_{-0.03}$	$1.63^{+0.04}_{-0.04}$
$\chi^2/d.o.f.$	2.61	2.29

- Power index $\Gamma = 3.5 \pm 0.1$
- $\{\mathrm{EM} \quad \text{and} \quad R \simeq 3.6\ \mathrm{pc}\ \} \Rightarrow n_{\mathrm{CSM}} \lesssim 0.6\ \mathrm{cm}^{-3}$

The NEI best-fit abundances

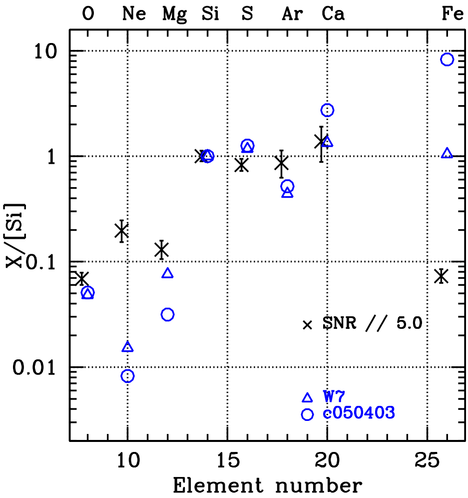

Abundances of thermonuclear explosion models:

- deflagration W7 (Nomoto et al, 1984)
- delayed-detonation c050403m (Woosley et al, 2007)

(include swept up $\sim 0.7\,M_\odot$ ejecta and shocked LMC circumstellar medium).

$[O-Mg]$ — overestimated
$[Fe]$ — underestimated
(Hughes et al 1998)

The NEI best-fit abundances

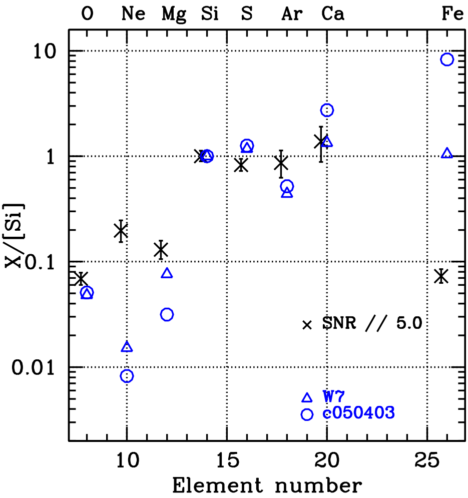

Abundances of thermonuclear explosion models:

- deflagration W7 (Nomoto et al, 1984)
- delayed-detonation c050403m (Woosley et al, 2007)

(include swept up $\sim 0.7\,M_\odot$ ejecta and shocked LMC circumstellar medium).

$[O - Mg]$ — overestimated
$[Fe]$ — underestimated
(Hughes et al 1998)

RGS spectra

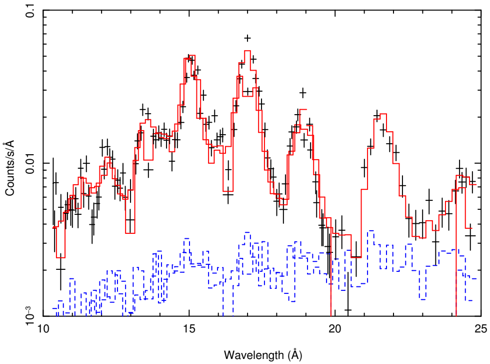

0.5 - 1.2 keV; NEI fit

$kT_e = 0.75 \pm 0.3$ keV

$\sigma_v = 5000 \pm 400$ km/s

N — is not the product of SNIa explosion, but comes from the shocked CSM

$n_{CSM} = (0.4 - 0.7)\ \mathrm{cm}^{-3}$

RGS spectra

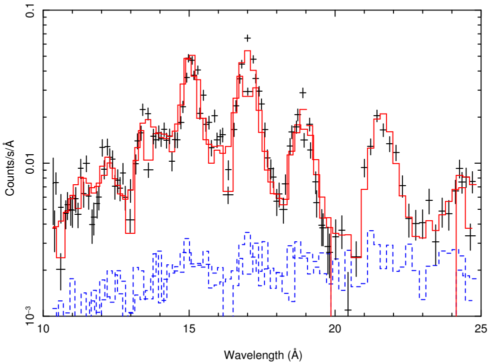

0.5 - 1.2 keV; NEI fit

$kT_e = 0.75 \pm 0.3$ keV
$\sigma_v = 5000 \pm 400$ km/s

N — is not the product of SNIa explosion, but comes from the shocked CSM

$n_{\rm CSM} = (0.4 - 0.7)\ {\rm cm}^{-3}$

RGS spectra

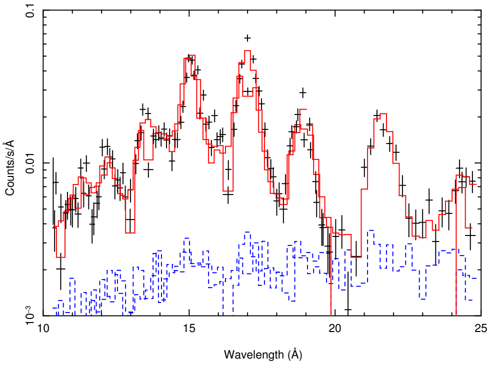

0.5 - 1.2 keV; NEI fit

$kT_e = 0.75 \pm 0.3$ keV
$\sigma_v = 5000 \pm 400$ km/s

N — is not the product of SNIa explosion, but comes from the shocked CSM

$n_{CSM} = (0.4 - 0.7)$ cm^{-3}

RGS spectra

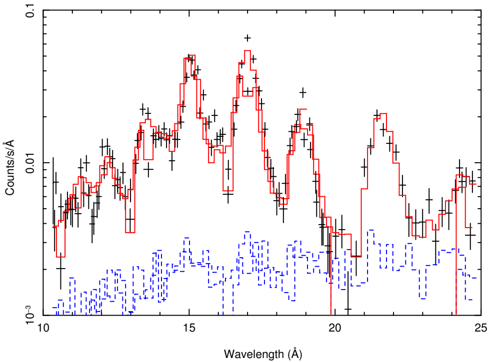

0.5 - 1.2 keV; NEI fit

$kT_e = 0.75 \pm 0.3$ keV
$\sigma_v = 5000 \pm 400$ km/s

N — is not the product of SNIa explosion, but comes from the shocked CSM

$$n_{\rm CSM} = (0.4 - 0.7)\ {\rm cm}^{-3}$$

Numerical method

Second approach:
Hydrodynamical model + synthetic X-ray spectrum
SUPREMNA hydrocode (Sorokina et al, 2004)

1D (spherical symmetric), but

- self-consistent account for time-dependent ionization
- difference in temperatures of electrons and ions
- the influence of radiative losses
- the account of electron thermal conduction
- the account of nonthermal particles
- inner-shell collisional ionization

Numerical method

Second approach:
Hydrodynamical model + synthetic X-ray spectrum
SUPREMNA hydrocode (Sorokina et al, 2004)

1D (spherical symmetric), but

- self-consistent account for time-dependent ionization
- difference in temperatures of electrons and ions
- the influence of radiative losses
- the account of electron thermal conduction
- the account of nonthermal particles
- inner-shell collisional ionization

Theoretical models of SNIa

W7:

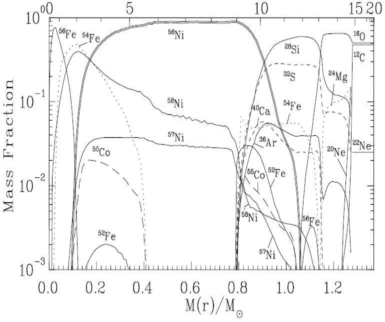

c70103m:

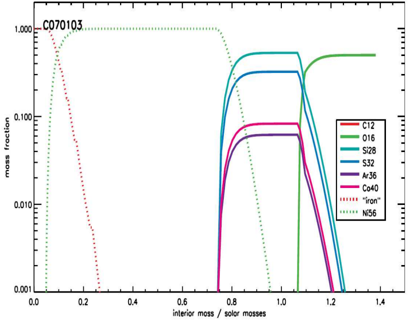

Theoretical models of SNIa

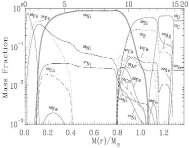

W7

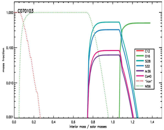

c70103m

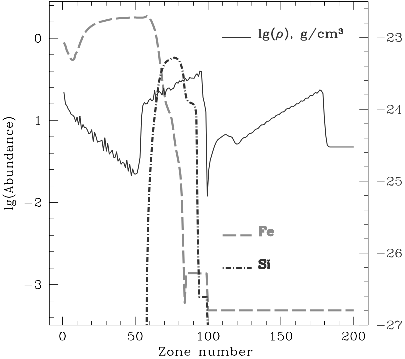

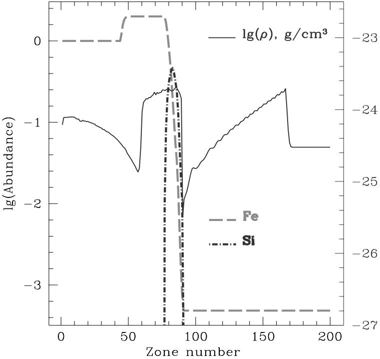

X-ray spectra, based on HD simulations

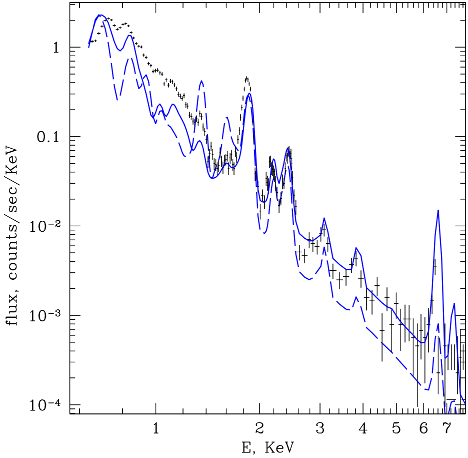

$\rho_{\rm CSM} = 3 \times 10^{-25}$ g/cm^3

$t = 400$ years

- W7
  $E = 1.2 \times 10^{51}$ erg
  dashed,
  $\chi^2/d.o.f. \simeq 21$
- c050403
  $E = 1.4 \times 10^{51}$ erg
  solid, $\chi^2/d.o.f. \simeq 13$

the lack of the Fe L emission is due

to incomplete Fe XVII atomic data

X-ray spectra, based on HD simulations

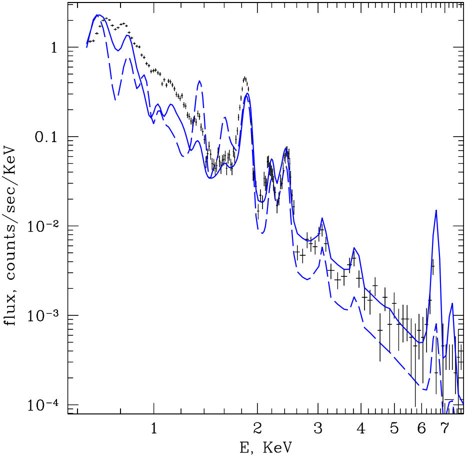

$\rho_{\rm CSM} = 3 \times 10^{-25}$ g/cm^3

$t = 400$ years

- W7
  $E = 1.2 \times 10^{51}$ erg
  dashed,
  $\chi^2/d.o.f. \simeq 21$
- c050403
  $E = 1.4 \times 10^{51}$ erg
  solid, $\chi^2/d.o.f. \simeq 13$

the lack of the Fe L emission is due to incomplete Fe XVII atomic data

Overview of SNR 0509-67.5

SPEX fitting and numerical simulations

Parameters	R, pc	t, yrs	n_{CSM} cm^{-3}	σ_v, km/s	kT_e, keV	kT_i, keV	$M_{Fe}, M_\odot$
SNR 0509-67.5	3.6	$\lesssim 500$	$0.4 - 0.6$	5000 ± 400	$1.0 - 4.0$	~ 70	~ 0.05
W7	3.6	400	0.4	$\lesssim 4300$	$1.8 - 1.9$	$20 - 36$	~ 0.12
c050403m	3.8	400	0.4	$\lesssim 4700$	$2 - 45$	$30 - 300$	~ 0.36

Data analysis and the simulations:

- $R \simeq 3.6$ pc,
- $t = 350 - 400$ years,
- $\sigma_v \simeq 5000$ km/s
- $n_{CSM} \simeq 0.4$ cm^{-3}
- $T_e/T_i \sim 0.01$
- Iron-rich progenitor, with an explosion energy $E = 1.4 \times 10^{51}$ ergs

Overview of SNR 0509-67.5

SPEX fitting and numerical simulations

Parameters	R, pc	t, yrs	n_{CSM} cm^{-3}	σ_v, km/s	kT_e, keV	kT_i, keV	$M_{Fe}, M_\odot$
SNR 0509-67.5	3.6	$\lesssim 500$	$0.4 - 0.6$	5000 ± 400	$1.0 - 4.0$	~ 70	~ 0.05
W7	3.6	400	0.4	$\lesssim 4300$	$1.8 - 1.9$	$20 - 36$	~ 0.12
c050403m	3.8	400	0.4	$\lesssim 4700$	$2 - 45$	$30 - 300$	~ 0.36

Data analysis and the simulations:

- $R \simeq 3.6$ pc,
- $t = 350 - 400$ years,
- $\sigma_v \simeq 5000$ km/s
- $n_{CSM} \simeq 0.4$ cm^{-3}
- $T_e/T_i \sim 0.01$
- Iron-rich progenitor, with an explosion energy $E = 1.4 \times 10^{51}$ ergs

Conclusions

- First approach: Single ionization timescale NEI fitting helps to estimate and constrain the basic features of the SNR.
- Second approach: With the knowledge of this basic features we can produce a self-consistent numerical model of the remnant for more thorough investigation.